REMOVAL OF HEAVY METAL FROM WASTE WATER BY ADSORPTION USING CHEM-BIO MODIFIED BIO DEGRADABLE WASTE WITH THE HELP OF SILVER NANO PARTICLES FROM SYZYGIUM CUMINI SEEDS EXTRACT

*1*Vani Shanmuganathan,** 2Manivannan-R
*1Department of Chemistry GCW Kumbakonam, **2Department of Chemistry GCM Kumbakonam,

AIM AND OBJECTIVES

The main aims of this research study are to assess the capability of Syzygium Cumini seeds extract act as a 'phytoremediator' to remove (or to decrease)Heavy metal pollution in water and to find a useful function for the biomass generated. In this process the author would fulfil the objectives mentioned below.

a.Heavy metals absorptions and analysis techniques

b. Nanoparticles formation and their further industrial use

c. Biomass formation from SC plants, their use and disposal methods Significance of the study.

Key Words: SC- Syzygium Cumini, AgNo3- Silver Nitrate, NP-Nano particles, Jamun –Syzygium cumini.

INTRODUCTION

Water pollution is one of the most serious problems because inorganic and organic wastes are discharged to the aquatic environment either in water soluble or insoluble forms [1,2]. Among the inorganic pollutants, heavy metals are the most serious because they are non-biodegradable and have the ability to accumulate in living organisms. Lead and cadmium are considered the most toxic and hazardous to the environment [3,4]. Lead is currently implemented in a significant number of industries such as cables, batteries, pigments, paints, steels and alloys, metal, glass, and plastic industries [5]. The discharge of these industries causes the contamination of the aquatic environment by lead. On the other hand, the exposure to cadmium may cause hypertension, hepatic injury, renal dysfunction, teratogenic effects, and lung damage [3,6].

The removal of heavy metals is considered an important issue with respect to the environment and economical considerations. There are several methods for the removal of heavy metals from aqueous solution including, adsorption on activated carbon, reverse osmosis, ion exchange, chemical precipitation, and membrane filtration [7,8]. However, the feasibility of economical and technical factors may limit the implementation of these methods [3].

One of the emerging and attractive technologies to remove heavy metals from aqueous solution is the biosorption process. Various biomasses such as bacteria [9], yeast [10], fungi [11,12], and algae [13–16] plants and seeds extracts were investigated as biosorbent for the removal of heavy metals. The aforementioned articles

demonstrated that SC Seeds extract biosorbent might be effective, in particular, when they are existed in dead cells form. SC SEEDS biosorbent seem to be more promising than macroalgae (seaweeds).

Removal of heavy metals from wastewaters [17–19]. Syzygium cumini seeds extract have some advantages over other Plants including their greater volume with high binding affinity, large surface area, and simple nutrient requirements [20]. SC seeds are easily cultivated in a large scale in environmental and in laboratory cultures providing a low cost biomass for the biosorption process. The present work was designed to investigate the biosorption behavior of Pb and Cd to the SC seeds .

MATERIAL AND METHODS

Materials preparation

Syzygium Cumini was collected from Alavandhipuram Cauvery River Delta (papanasam taluk) Thanjavore District, during the month of July-2015. The collected plants.were stored by refrigerator to continue my further studies.

These washed SC seeds with distillated water to clean the surface pollutants and dried in the air and absence of sunlight at the Lab. temperature (27 ± 2 °C). The dried seeds were milled by electric milling and sieved to powders. 5 g of powders were introduced to 100 ml of distilled water in the beaker and heated to 80 °C for 15 min. After cooling to Lab. temperature filtered with 0.45 µ filter paper. This solution as capping agent was maintained in the refrigerator for further use.

Preparation of silver nitrate solutions:

The molecular weight of the Silver nitrate-169.86gm was weighed per litre. This method was prepared by one molar silver nitrate solution each. In other method of preparation 1mM solution of silver nitrate was weighed by 0.169.86 mg/liter. The Erlenmeyer flask 2 (250 ml) containing 100 ml each de-ionized water for dissolved AgNO3 salts for preparation of 1mM silver nitrate solutions.

Extraction and fractionation of S. cumini seeds:

The collected plant's seeds(Syzygium cumini) were identified by "The Botany Herbarium"(Departments of Zoology), Govt women college(Autonomous), Kumbakonam. The seeds of the plant S. cumini were thoroughly washed and dried at 370 C. The dried seeds were further pulverized into fine powder. 25gm of the powdered seed was taken for the extraction purpose in ethanol as the solvent, by using Soxhletor apparatus. This seed extract (Sc) was used for studying the various antioxidant assays. The 5 gm of seeds (Syzygium cumini) were taken into an Erlenmeyer flask with 100 ml of sterile de-ionized water. The mixture was boiled for 5-10 min at 100ºC; finally the mixture was filtered and stored at 4°C for further studies.

Biosynthesis of Silver Nanoparticles from S. cumini Seed (ScSNPs):

A measured quantity of finely powdered seed (5gm) was mixed with 100mL of deionized water and then boiled the mixture for 5 min before finally decanting it. This suspension was then centrifuged at 5,000 rpm for 15 minutes at 40 C using fresh deionized water. The extract volume was adjusted to an appropriate volume by adding deionized water, and filtered through Whatman filter paper No.1. 10 mL of seed extract was added to 90 mL of 1 mM aqueous AgNO3 solution for reduction of Ag+ ions and incubated at room temperature in dark condition for 24 hours. Thesolution was then centrifuged at 10,000 rpm for 20min to separate the silver nanoparticles. These silver nanoparticles were washed three times with deionized water and stored as

lyophilized powder.

In vitro Antioxidant Assays:

Determination of Total Phenolic Content:

The total phenolic content was determined by the Folin-Ciocalteau method [19, 20]. The total phenolic content was expressed in terms of Gallic acid equivalent (mg/g of dry mass).

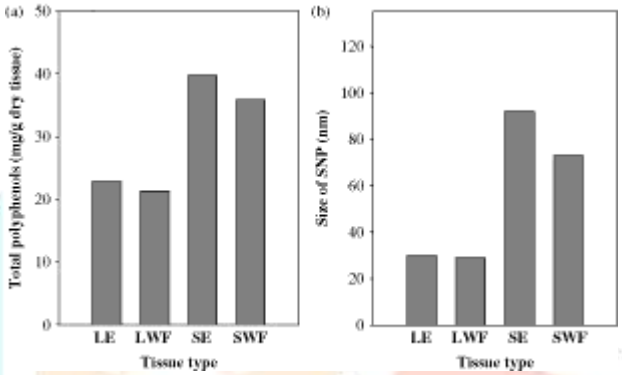

DPPH Free Radical Scavenging Assay:

The DPPH free radical scavenging assay was carried out by the method of Tagashira et al., [21] and Chang et al., [22]. The percentage of inhibition or scavenging of free radicals was determined by the formula % Inhibition= [(Control OD – Sample OD)/ Control OD] * 100, where control was prepared as above without extract.

Reducing Power Assay:

The reducing power assay was carried out by the method of Koleva et al., [41] and Makari et al., [42]. Ascorbic acid was used as standard and phosphate buffer used as blank solution. Increased absorbance of the reaction mixture indicates stronger reducing power.

Total Antioxidant Capacity:

The total antioxidant capacity was assayed following the method of Preito et al., [25]. Ascorbic acid was used as the standard and the total antioxidant capacity was expressed as equivalents of ascorbic acid.

Statistical Analysis:

All the grouped data were statistically evaluated by using Student't test with SPSS/16 software. P values of less than 0.05 were considered to indicate statistical significance. Values are presented as the mean ± S.D. of each three replicates in each experiment.

Silver particles were also synthesized by wet chemical co-precipitation method :

(The term "wet chemical methods" emerged in contrast to conventional and solid-state synthesis methods of compounds and materials widely used also in ceramics manufacturing. Today the term refers to a

group of methods of powder and material production (liquid phase sol-gel process, hydrothermal synthesis, Pechini method, spray drying, aerosol spray pyrolysis, cryochemical synthesis, etc.) using liquid phase at one of the process stages. The main differences between wet chemistry products and similar products of solid-phase synthesis are much smaller grains (crystallites) and, usually, lower temperature and shorter duration of phase formation.)Adapted from Moghaddam et al, [43].

The beaker containing 0.9 M aqueous solution of sodium hydroxide was heated at 55ºC followed by drop wise addition of 0.45 M aqueous solution of silver nitrate(Ag(NO3)2.4H2O) under speed stirring. The precipitates of Ag nanoparticles were collected after 2 hours standing, cleaned with distilled water, ethanol and finally air dried at 60 ºC.

Characterization:

Each synthesized silver nanoparticle was subjected to characterization by standardized spectroscopic tools of Fourier Transform Infrared (FTIR) and UV-Visible spectroscopy. FTIR spectra of pressed pellet were recorded from 4000 cm-1 to 400 cm-1 on FTIR-8400, Shimadzu, Japan. The dried mass of SC seed extract (reducing agent) was also pressed into pellet for observation under FTIR. UV-VIS spectra were fit with Gaussian curves for measurement of λmax keeping distilled water for background correction. The samples surface morphology and size was determined with Scanning Electron Microscopy (SEM) coupled with EDX. Sample was sonicated and analyzed at different magnifications on 6490(LA) JEOL machine with gold sputtering at a potential of 20 kV prior to recording SEM. EDX analysis was done on JED-2300 analysis station.

Figure 1 Syzygium cumini seeds extract sample

Figure 2 Change in the color of the solution from brown to dark brown.

Figure 3 Silver nitrate solution, reaction mixture change in the color of the solution

Metal solutions standards

Metal salts used in the preparation of the synthetic metal bearing solutions were $CdCl_2 \cdot 5/2H_2O$,$Pb(NO3)_2$, $CrO2$.The synthetic wastewater solutions were then prepared by diluting the stock standards of concentration 1000 mg/L of each metal. Deionized water was used in all experiments.

Analytical methods

Determination of metals concentration

The concentrations of metals in all samples were determined according to the APHA method [22] using Atomic Absorption Spectrometer (Varian SpectrAA 220, USA) with graphite furnace accessory and equipped with deuterium arc background corrector. Precision of the metal measurement was determined by analyzing the metal concentration of all samples.

Batch Experiment for Adsorption:

The synthesized silver nanoparticles (NPs) were applied as adsorbents in time-dependent batch experiment to evaluate the removal of Pb II Cd II and Cr IV. Each batch was investigated at variable temperature and pH to determine the optimal removal efficiency. The following general protocol is adopted for batch experiment.

Synthetic solution of known concentration (0.01 mg/L) of each Pb II Cd II and Cr IV was prepared and a known volume (5ml) of it was added in test tubes containing 1mg of each adsorbent.The aliquot was drawn after 5 minutes, filtered and analyzed on UV-visible spectrophotometer at wavelengths of 250 nm, 260 nm and 241 nm for phenanthrene, anthracene, and pyrene, in respective order.

Quality control

For each series of measurements, absorption calibration curve was constructed composed of a blank and three or more standards. The accuracy and precision of the metals measurement were confirmed using external standard reference material 1643e for trace elements in water and quality control sample from National Institute Standards and Technology (NIST).

Batch biosorption studies

Each of the batch biosorption studies was carried out by contacting the SC seeds extract with the metal ions in 250 ml stopper conical flask. The experiments were conducted at room temperature (25 ± 0.1 °C) to determine the effects of pH, biosorbent dosage, contact time, and initial ions concentration on the biosorption of Cd(II), Pb(II) and Cr(IV) ions. Each experiment was conducted in a mechanical shaker at 120 rpm. The samples were filtered through Whatman filter paper (No. 41) and the metal ions concentration was determined in the filtrate. To distinguish between possible metal precipitation and actual metal sorption, controls (blank) were used without biosorbent materials.

All the experiments were carried out in triplicate and the mean of the quantitative results were used for further calculations. For the calculation of mean value, the percent relative standard deviation for results was calculated and if the value of standard deviation for a sample was greater than 5%, the data were discarded .

Effect of pH

The batch experiment was carried out by contacting 0.1 g of SC Seeds extract with 100 ml of 50 mg/L of metal solution in 250 ml stopper conical flask at different pH value, ranging from 2 to 6 (below 2, the high proton concentration minimizes the metal sorption and above 6 the metal precipitation is favored). The pH of the solutions was adjusted either by hydrochloric acid or sodium hydroxide. The mixture was shaken for 2 h at room temperature, filtered, and the final pH for each sample was determined.

Effect of contact time

The optimum time was carried out at optimum pH by conducting batch biosorption experiments with an initial metals ions concentration of 50 mg/L, 10 g/L biosorbent dosage and at different time periods (5, 15, 30, 60, 90, 120 min).

Effect of biosorbent dosage

The biosorbent dosage varied from 0.025 to 0.25 g using a fixed volume of 100 ml of 50 mg/L of metal solution at the optimum pH and the equilibration time for each metal.

Biosorption isotherms

Isotherms were measured by varying the initial metal ion concentrations at the optimum conditions for each metal. Different biosorption models were used for comparison with experimental data [23].

RESULTS AND DISCUSSION

The biosorbent used in this study was Syzygium cumini seeds extract (SC Seeds) collected from Alavandhipuram Cauvery River Delta (papanasam taluk) Thanjavore District Fig. 1 shows that, there are different shapes of SC Seeds NPs such as filament solitary or free clusters, the cells were cylindrical barrel-shaped or spherical and the terminal cells were spherical or slightly elongated. The spherical heterocysts were elongated and slightly greater than vegetative cells due to nitrogen fixation (Fig. 5).

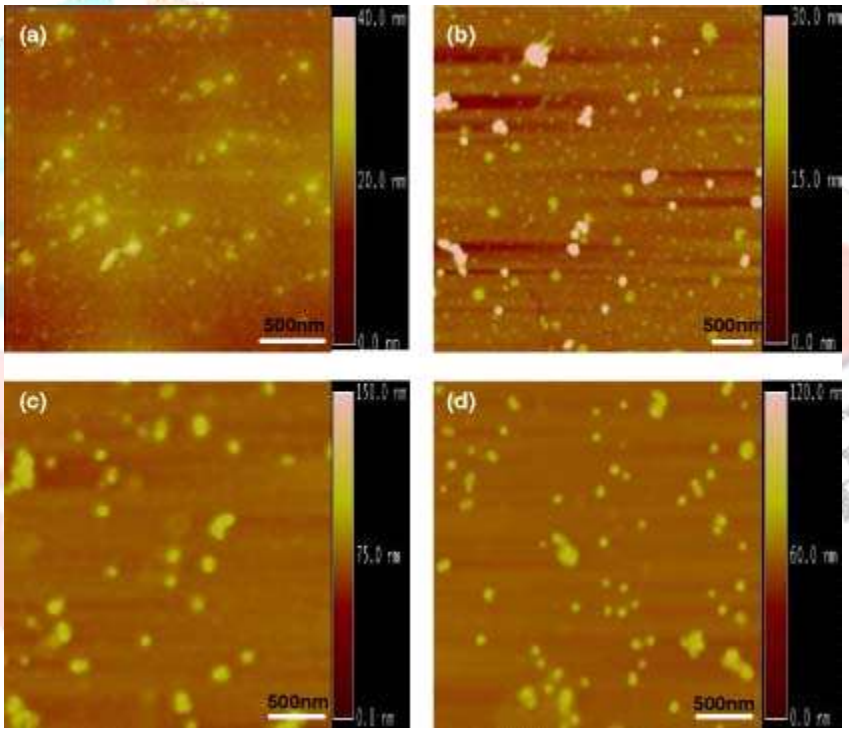

Figure 4 SC Seeds NPs such as filament solitary or free clusters, the cells were (a) cylindrical barrel-shaped or (b) spherical and the(c) terminal cells were spherical or (d) slightly elongated

Characterization of dried biosorbent

The results illustrated in Fig. 2 showed the FTIR spectra of the unloaded biomass and Pb(II)-loaded biomass. These results represented the information about the functional groups on the surface of the cell wall of the biomass and the possible interaction between metals and the functional groups. From these data, it is clear that the strong and broad band at 3393 cm−1 might be related to the overlapping between N—H and O—H stretching vibration. However, the band at 2924 cm−1 could be related to the —CH stretch and the band at 1646 cm−1 could be assigned to asymmetric stretching vibration of CO. On the other hand, the intense and strong band at 1053 cm−1 might be attributed to the stretching of C—O group on the surface of the biomass [3]. Meanwhile, some bands in the fingerprint region could be related to the phosphate groups. It could be observed that the bands at 3425, 3751, 2943, 1729, and 580 cm−1 were shifted to 3410, 2943, 1622, 1077, and 556 cm−1

after loading of Pb(II). The significant changes in the wave number of these peaks after loading of Pb(II) indicate that the functional groups (amido, hydroxyl, CO and C—O) were involved in the biosorption of Pb(II) on the surface of A. sphaerica. Similar results for the biosorption of heavy metals on different species of algae have been previously reported by others [3,24,25].

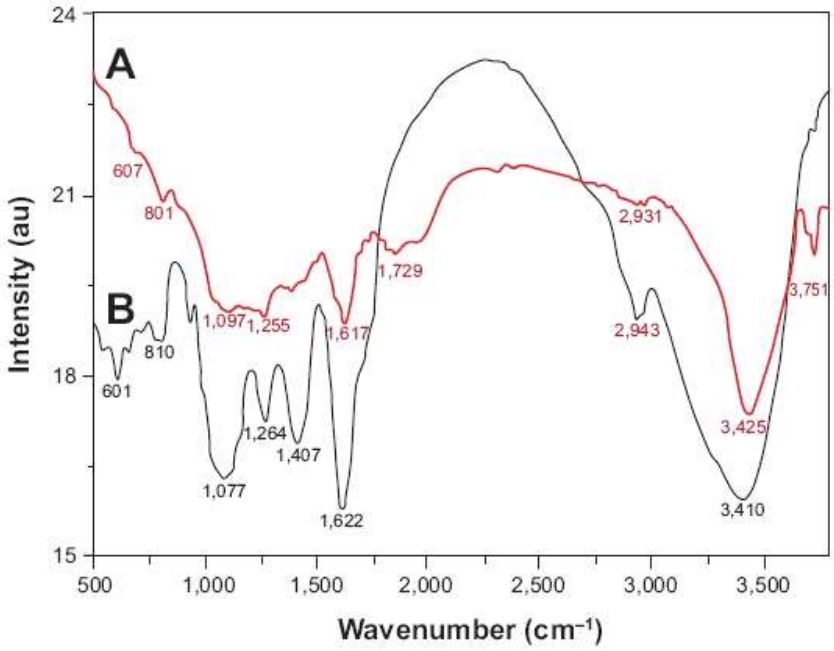

Figure 5 Fourier-transform infrared spectra of pure green synthesized silver nanoparticles (Ag-nanoparticles-plant extract) (line **A**) and Syzygium cuminiplant extract (line **B**).
Note: The similarities between the spectra strongly suggest the presence of plant extract residue in the Ag-nanoparticles-plant extract as a capping or stabilizing agent.

Optimum conditions

Effect of pH

It is well documented that the pH of the aqueous solution affects the metal solubility and the concentration of the counter ions on the functional group of the cell wall of the biosorbent, consequently, the pH is considered as the most important parameter that could affect the biosorption of metal ions from solutions [26,27]. The effect of pH value on the biosorption of Cd(II), Pb(II) and Cr(IV) ions onto SC Seeds extracts was evaluated and the results were presented in Fig. 6. It is clear that the maximum biosorption for Cd (II), Pb(II) and Cr(IV) reached 84.5%, 88.3% and 86.2% at pH 5.5 . 5.07,and 7, respectively. Therefore, all the experiments were carried out at pH 5.5 for Cd ,5.07 for Pb and 7 for Cr IV.

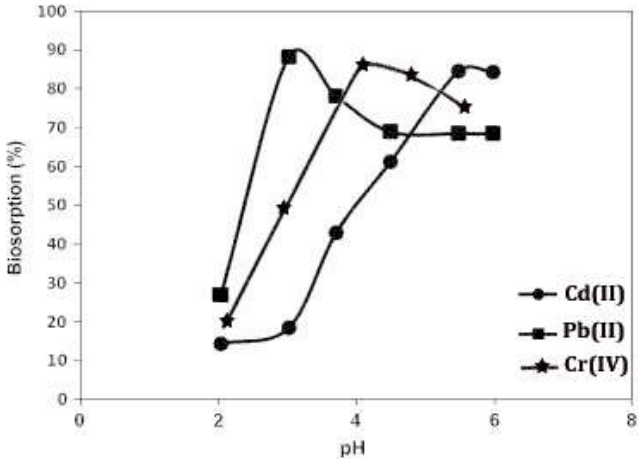

Figure 6 Effect of pH

The current results indicated that the biosorption of Cd(II), Pb(II) and Cr(IV) was increased with increasing the pH value. This is because, at lower pH, the concentration of positive charge (protons) increased on the sites of biomass surface, which restricted the approach of metal cations to the surface of biomass (because of charge repulsion) [28]. As the pH increase, the proton concentration decreases and the biomass surface is more negatively charged. The biosorption of the positively charged metal ions increased till reaching their maximum biosorption around pH 5.5 and 3 for Cd(II), Pb(II) and Cr(IV) respectively. The maximum biosorption efficiency of Cd(II), Pb(II) and Cr(IV) was occurred at different pH values. This could probably correlate to the different characteristics between the metals (size, electronegativity), or the more available metal was better biosorbed on the adsorption sites [2]. For Pb(II), the maximum biosorption at lower pH is related to its higher electronegativity than Cd and cr(IV), so Pb affinity to the surface functional groups of the cell wall is higher than Cd and cr(IV) at low pH value. While, the decrease in biosorption yield at higher pH not only related to the formation of soluble hydroxilated complexes of the metal ions (lead ions in the form of Pb(OH)2 [29], but also to the ionized nature of the cell wall surface of the biomass under the tested pH. Also, the main cadmium cation sequestration mechanism by the algal biomass was apparently chelation, while lead cations exhibit higher affinity to the algal biomass, and their binding mechanism include a combination of ion exchange, chelation, and reduction reactions, accompanied by metallic lead precipitation on the cell wall matrix [29].

Effect of biosorbent dosage

Different biomass dosage ranged from 0.025 to 0.25 g/100 ml was applied to study the effect of biomass dose on the biosorption of Cd(II), Pb(II) and Cr(IV) ions Fig. 7. The data revealed that the biosorption efficiency of Cd(II), Pb(II) and Cr(IV) ions on SC seeds was significantly affected by the dose of SC Seeds extract in the solution. In other words, the biosorption of Cd(II), Pb(II) and Cr(IV) ions was increased with subsequent increasing the biosorbent dose and almost became constant at higher dosage than 0.1 g/100 ml and 0.2 g/100 ml for Pb and Cd, respectively. This behavior could be explained by the formation of aggregates of the biomass at higher doses, which decreases the effective surface area for biosorption [3,30]. Therefore; the doses 0.1 g/100 ml for Pb(II) and 0.2 g/100 ml for Cd(II) were selected as the optimum doses of the biosorbent for the rest of the study.

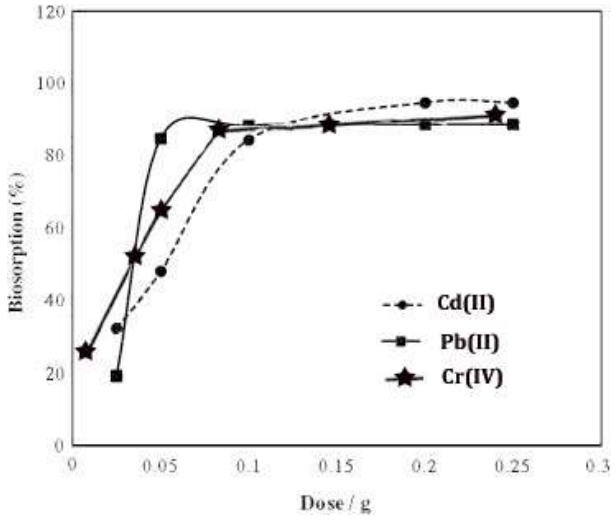

Figure 7 biosorbent dosage

Effect of contact time

The effect of contact time is highly influencing the biosorption process. Fig. 8 showed the effect of contact time on the biosorption of Cd(II), Pb(II) and Cr(IV) ions using the SC Seeds extract. These results indicated that the biosorption of three metals was rapid in the first 20 min then was gradually increased till the equilibrium attained at 60 and 90 min for Cd(II), Pb(II) and Cr(IV), respectively, and the biosorption became almost constant thereafter. Therefore, a contact time of 60 and 90 min was used as the optimum time for Cd(II), Pb(II) and Cr(IV) for the rest of experiments. The rate of biosorption of Cd(II), Pb(II) and Cr(IV) ions using the SC Seeds Extracts seems to occur in two steps; a very rapid surface biosorption in the first step and a slow intracellular diffusion in the second step. In this concern, Chen et al., [2] reported similar behavior for the biosorption of Ni and Cu on treated alga Undaria pinnatifida and the adsorption of Cd by biomass fungal biosorbent [31].

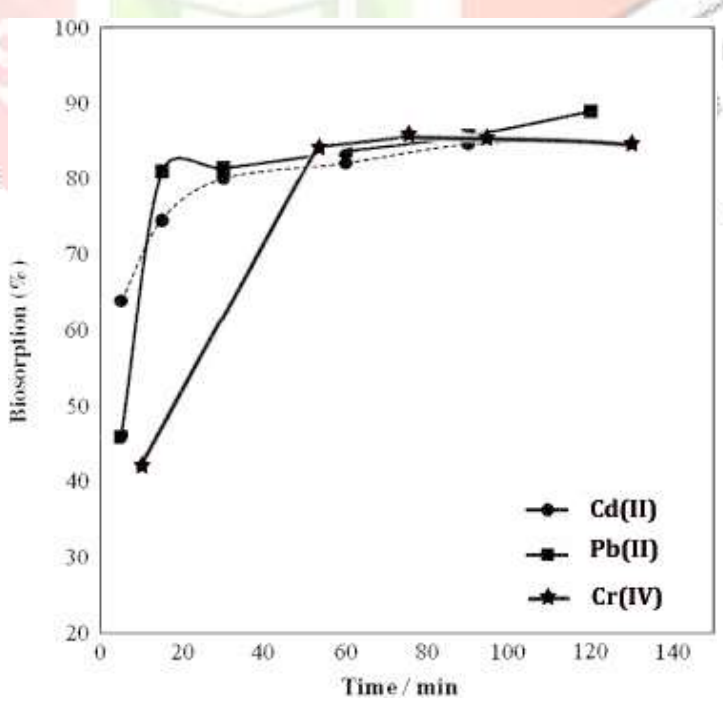

Figure 8 Effect of Contact Time

Effect of metal concentration

The data presented in Fig. 9 showed the effect of metal concentration on biosorption process. The concentration of Cd(II), Pb(II) and Cr(IV) were varied between 50 and 300 mg/l at the optimum pH, contact time, and optimum dose for each metal, respectively. The results presented in Fig. indicated that the biosorption of Cd(II), Pb(II) and Cr(IV) at the beginning was 83%, 70.72%, and 79% respectively. The biosorption was decreased with increasing the metal concentration. This behavior was attributed to the fact that, initially, all binding sites on the biomass surface were vacant resulting in high metal biosorption at the beginning. After that, with increasing metal concentration, the biosorption of metal was decreased because of a few active sites were available on the surface of the algal biomass.

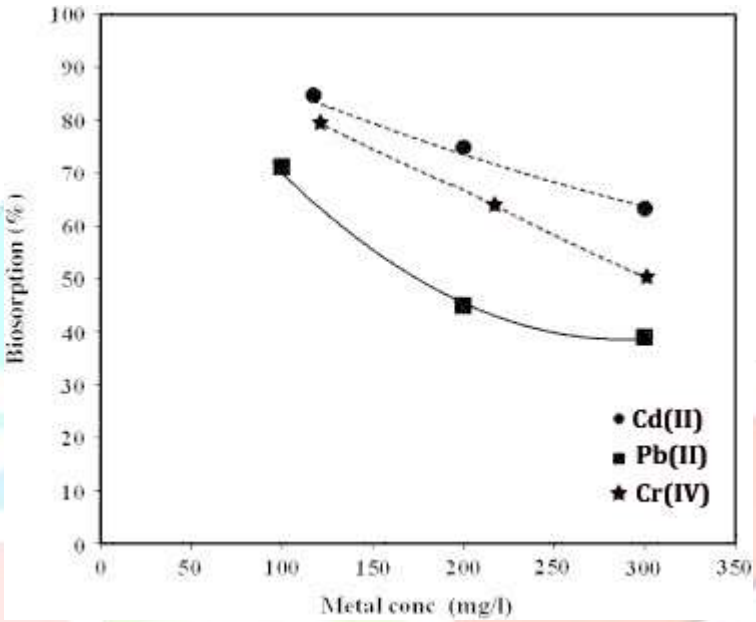

Figure 9 Metal Conc

Adsorption isotherms

An adsorption isotherm is a good tool for understanding the nature of the surface of the biosorbents..

The biosorption data have been subjected to different biosorption isotherms, namely, Langmuir, Freundlich, Temkin and Dubinin–Kaganer–Radushkevich (DKR) (Table 4).

The Langmuir isotherm constant KL and qmax were calculated from the slope and intercept of the plot Ce/qe versus Ce. The maximum Cr(lV), Pb(II) and Cd sorption onto SC Ag Np was 16.07, 15.60, 15.87 mg g−1 respectively, with high value of correlation coefficient (R2). This indicates a good agreement between the parameters and confirms the monolayer biosorption of metal ions on the surface of both the adsorbents.A further analysis of the Langmuir equation can be made on the basis of dimensionless equilibrium parameter, RL (Hall et al. 1966) also known as separation factor, given by

RL= 1/1+bco

The value of RL lies between 0 and 1 indicating that the biosorption is favorable for both the adsorbents.

The Freundlich constants KF and n were calculated from the slope and intercept of the straight line plot lnqe versus lnCe. As it can be seen in Table 5, the values of n lies between 1 and 10 (i.e. 1/n < 1), representing a favorable sorption.

Table 1 *Various isotherm constants and correlation coefficients for the biosorption of Cr(IV), Pb(II) and Cd o*n SC Ag Np adsorbent dose = 1.5 g/0.1 L; pH = 2.0 for Cr(lI), pH = 6.0 for Pb(II) and pH = 4.0 for Cd

Adsorbent T	Metal ion	Langmuir isotherm constants			Freundlich isotherm constants		
		qmax (mg g-1)	K (L mg-1)	R2	KF (mg g-1)	n	R2
SC Ag Np	Cr(IV)	16.07	0.01	0.99	1.67	3.48	0.97
	Pb(II)	15.62	0.04	0.97	0.67	2.12	0.51
	Cd	15.85	0.03	0.99	0.04	1.82	0.95

In order to estimate the characteristic porosity of the biomass and apparent energy of biosorption, the Dubinin–Radushkevich model was used (Dubinin 1960). β is related to the free energy of sorption per mole of sorbate as it migrates to the surface of the biomass from infinite distance in the solution. The porosity parameter values β for the biomass towards the metal was less than unity indicating that sorption of Cr(II), Pb (II) and Cd onto SC Ag Np was significant (Table 1). Values of qm were also in accordance with the experimental data. R2values obtained from data also supported the fitness of model to sorbents.

In comparing the linear correlation coefficients of all the two isotherms (Table 1), it could be concluded that the biosorption of Cr(IV), Pb (II) and Cd onto SC Ag Np was best fitted to Langmuir isotherm under the concentration range studied confirming the monolayer biosorption.

Adsorption kinetics

Pseudo-first-order, pseudo-second-order, Elovich equation and intraparticle diffusion models were applied to study the reaction pathways and potential rate limiting steps of the biosorption of Cr(IV), Pb (II) and Cd onto SC Ag Np

Constants of pseudo-first-order, pseudo-second-order, were determined from the slope and intercept of the linear plot between log $(qe - qt)$ versus t and t/qt versus t, respectively (Table 2). Correlation coefficient for pseudo-first order was found to be appreciably high, but the calculated qe is not equal to experimental qe, suggesting the insufficiency of pseudo-first-order model to fit within the kinetic data. Pseudo-second-order equation showed excellent linearity with the experimental data with high correlation coefficient ($R2 > 0.99$) and the theoretical qe value is closer to the experimental qe value. So it was inferred that biosorption of Cr(II), Pb (II) and Cd onto SC Ag Np followed pseudo-second-order kinetics. This suggests that the rate limiting step of this sorption system may be chemisorption involving valency forces through sharing or exchange of electrons between adsorbent and adsorbate. A similar phenomenon was reported in the literature. (Jayaram and Prasad 2009; Lawal et al. 2010). Further, Elovich equation also supports chemisorption processes with high value of αand R2 obtained from the plot of qt versus lnt yielding a straight line.

Table 2 Parameters of various kinetic models for the biosorption Cr(II), Pb (II) and Cd on SC Ag Np adsorbent dose = 1.5 g/0.1 L; pH = 2.0 for Cr(II), pH = 6.0 for Pb(II) and pH = 4.0 for Cd

Adsorbent	Metal ion	Pseudo-first-order			Pseudo-second order		
		k1 (min-1)	Qe (mg g-1)	R2	k2 (min-1)	Qe(mgg-1)	R2
SC Ag Np	Cr(IV)	-5.7 9 10-3	2.76	0.98	0.0017	49.75	0.99
	Pb(II)	-6.7 9 10-3	2.72	0.90	0.0019	43.27	0.97
	Cd	-6.0 9 10-3	2.40	0.94	0.0016	37.89	0.95

In many biosorption processes, the adsorbate species are most probably transported from the bulk of the solution into the solid phase through intraparticle diffusion which is often the rate limiting step in many biosorption processes. So the intraparticle diffusion is another kinetic model which was used to study the rate of Cr(IV), Pb (II) and Cd biosorption on SC Ag Np. According to this model, if the plot of qt versus t0.5 gives a straight line, then the biosorption process is controlled by intraparticle diffusion. kp can be calculated from the slope of the plot of qt versus t0.5. Values of correlation coefficient are closer to unity which indicates the applicability of this model. The values of intercept give an idea about boundary layer thickness, i.e., the larger intercept, the greater is the boundary layer effect. The applicability of intraparticle diffusion model indicates that it is the rate limiting step (Kannan and Sundaram 2001).

In nutshell, it can be concluded that along with chemisorption, intraparticle diffusion are the rate limiting steps in the biosorption of Cr(IV), Pb (II) and Cd biosorption on SC Ag Np.

Biosorbent Regeneration

In this study 0.1 N HCl and 0.1 N NaOH were selected to desorb Cr(II), Pb (II) and Cd from exhausted SC Ag Np. Low desorption was obtained with NaOH as compared to HCl indicating that in acidic conditions, heavy metal cations are displaced by protons from the binding sites. Further the regeneration efficiency decreased from 92.63 % (in first cycle) to 45.23 % (in third cycle) in case of Cr(IV) for SC Ag Np 76.11 to 35.85 % for. Similar was the case for Pb(II) and Cd II metal ions. The complete desorption of the above said metal ions could not be obtained even with 0.5 N HCl, which might be due to the metal ions being trapped in the intrapores and therefore difficult to release (Al-Asheh and Duvnjak 1997).

UV-Vis Spectral Analysis

syzygium cumini seed extract was able to synthesize the silver nanoparticles by the indication of suitable surface Plasmon resonance (SPR) with peaks near visible spectrum at 420 nm (Figure 10). The absorbance peak near 420 nm, can be attributed to the plasmonic peak of silver nanoparticles, formed in the reaction mixture.

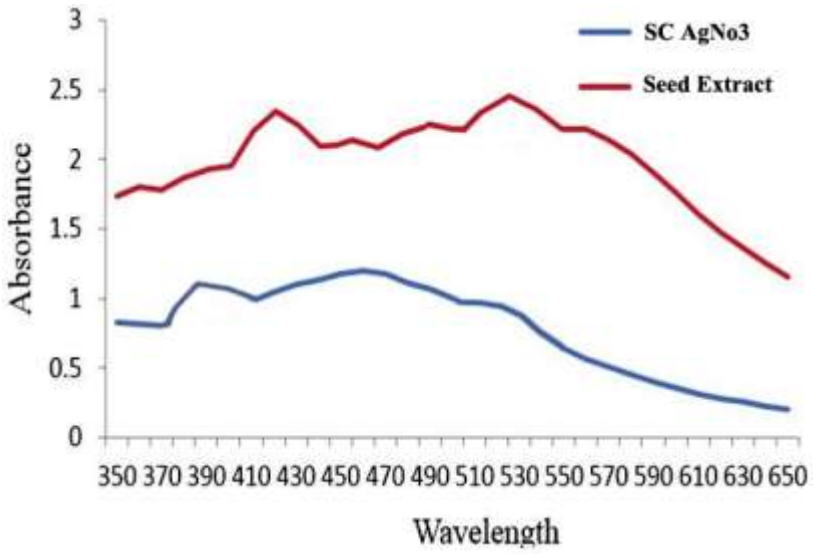

Figure 10 UV-Visible spectrum of biogenic silver nanoparticles.

Dynamic Light Scattering (DLS) Analysis

Figure 5 showed the DLS pattern of suspension of silver nanoparticles synthesised using Sc Seed extract. The size distribution profile indicates that the size of these silver nanoparticles showed two peaks at 5.23 nm (20%) and 77.82 nm (80%). Polydisperse index (PDI) of silver nanoparticles suspension is 0.332 indicating that synthesised particles are more or less homogeneous.

Zeta Potential Measurement

Silver nanoparticles synthesised by green method are stable in nature even after three months storage at room temperature as it showed zeta potential – 22.2 mV shown in Fig. 11. The negative zeta potential value indicated that these are highly stable due to the capping of biomolecules present in the flower extract. Measurement of zeta potential is depends on the movement of nanoparticles under influence of an applied electric field. The movement depends upon the surface charge and the local environment of the particle.

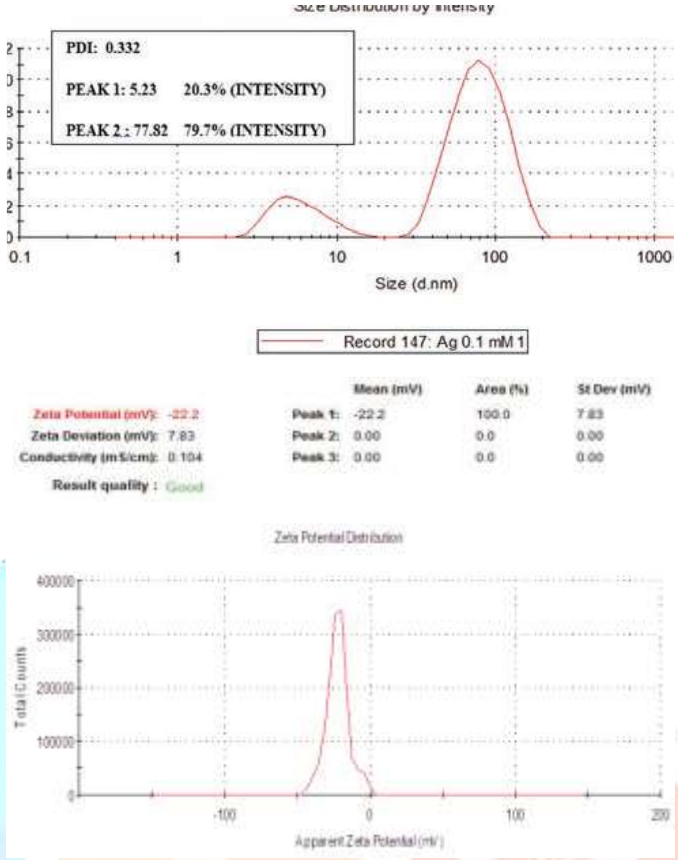

Figure 11 DLS pattern of biogenic silver nanoparticles and Zeta potential measurement.

Scanning Electron Microscopy Analysis:

`SEM analysis showed the image of high density AgNPs synthesised by Sc Seed extract (Fig. 12). From the given SEM image, it is concluded that the green synthesised silver nanoparticles are spherical in shape and without agglomeration. Formation of silver nanoparticles was due to interactions of hydrogen bond and electrostatic interaction between the biomolecules capping with Ag0 . The nanoparticles were not in direct contact, indicating stabilization of nanoparticles by capping agent.

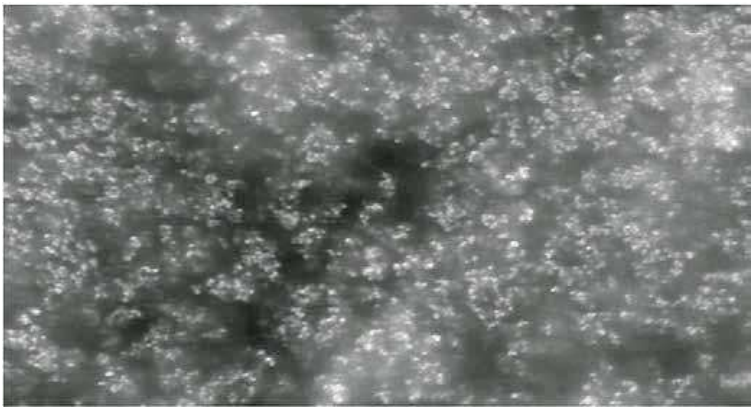

Figure 12 SEM image of biogenic silver Nano particles

Energy Dispersive Spectroscopic Analysis:

The EDX analysis was helpful in identifying the elemental composition of the synthesised nanoparticles. The obtained spectrum confirmed the presence of AgNPs (Fig. 13) in which the vertical axis displayed the x-ray counts and the horizontal axis displayed the keV. The identified line for the energy emission for Ag was shown and the peak was matched with the spectrum of Ag and correctly identified. The strong signal of silver has been detected in EDX indicating the purity of synthesised silver nanoparticles and thus giving confidence that silver has been correctly identified. The other signals available in EDX may be coming from the bioactive molecules in the Sc Seed's extract. Metallic silver nanocrystals generally showed typical optical absorption peak at 3 kev due to surface plasmon resonance. A sharp signal was observed at 3 kev also reported that distinctive peak for the absorption of crystalline nature of biogenic AgNPs.

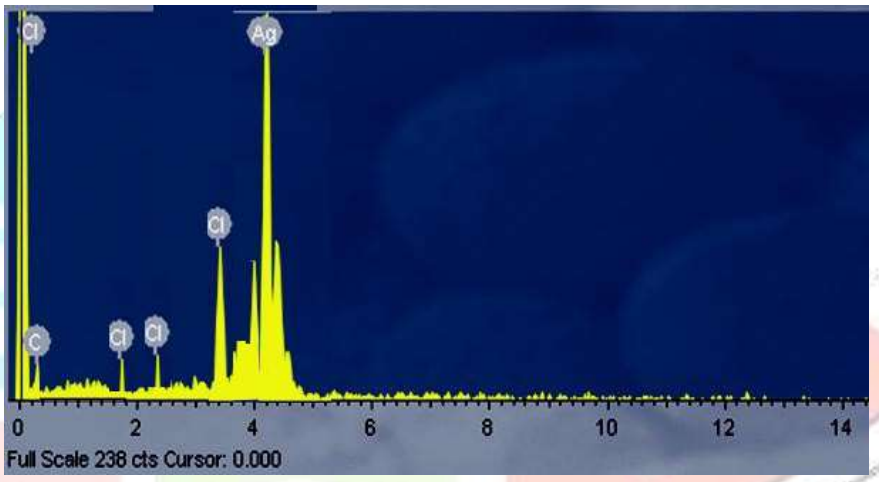

Figure 13 EDX

Atomic Force Microscopy Analysis:

To validate the surface morphology powder coated AFM images were taken in non- contact mode (Figs. 14(a) and 14(b)). Results showed variability in morphological features of Sc Seed's extract mediated silver nanoparticles and sizes varied from 20-70 nm. It is evident from the AFM images that particles are more or less homogeneous in size range and monodisperse nature.

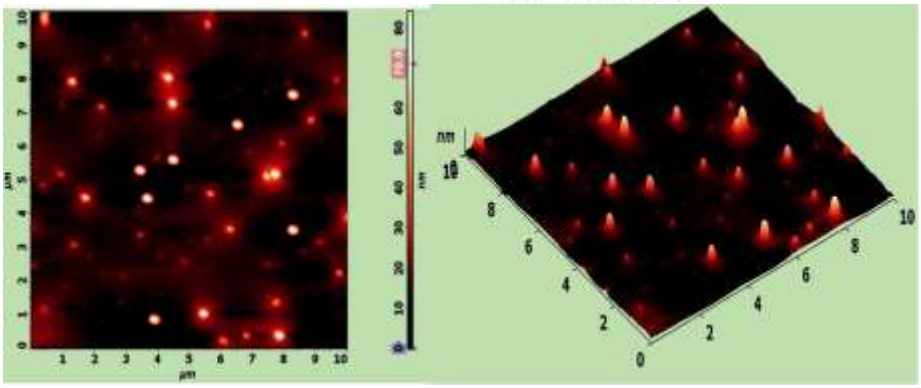

Figure 14 AFM

XRD Analysis

The XRD pattern was used to confirm the crystalline nature of the Sc Seed's AgNPs. Figure 10 showed the XRD pattern of the synthesised nanoparticles and main peaks corresponding to 2θ values of 27.80°, 32.27°, 38.20°, 44.02°, 46.57°, 64.52°, and 77.42° that could be indexed to (98), (101), (111), (200), (200), (220), (311) planes respectively. Similar results were obtained in leaf Clitoria ternatea extracts mediated AgNPs synthesis, in which 2θ values were obtained at 28.07°, 32.50°, 38.33°, 44.54°, 46.50°, 57.71°, 64.75°, and 77.69°22. The average size of nanoparticles determined by XRD was 12.5 nm (using Debye-Scherrer equation).

FT-IR Analysis

FTIR gives the information about the functional groups present in the synthesised AgNPs for understanding their transformation from simple inorganic AgNO 3 to elemental Ag by the action of different phytochemicals present in the seed extracts. In order to determine the functional groups on Tecomella flower extract, FTIR analysis was performed. The FTIR spectrum of syzygium cumini seed extract showed absorption band stretches at 3367-3315cm-1, 2927.94cm-1(C-H-Bond), 1647.21cm-1, 1325.10cm-1,1236.37cm-1, 1155.36cm-1 (C-O-Bond), 1018.41cm-1(C-N-Bond), 916.19cm-1 (C-H-Bond), 759.95cm-1 (C-H-Bond) and other stretches (Figure 11). The FTIR spectrum of syzygium cumini seed extract mediated silver nanoparticles showed (Fig. 12) absorption bands at 2939.52 cm-1(C-H-Bond), 2877.79 cm-1(C-H-Bond), 2362.8 cm-1, 1157.29 cm-1 (C-O-Bond), 1014.56 cm-1(C-N-Bond), 831.32 cm-1 (C-H-Bond), and 785.03 cm-1 (C-H-Bond).The characteristic of C-H bond, C-O bond and C-N bond stretching vibrations are common in both seed extract and seed extract mediated biogenic synthesised silver nanoparticles indicating that these biomolecules were involved in the reduction and capping of silver nanoparticles. C-H bond stretching mode found in alkane, C-O bond stretching mode of the carbonyl functional groups of esters and alcohols and C-N stretching bands are available in amine stretch of proteins and aminoacids present in seed extract of syzygium cumini.

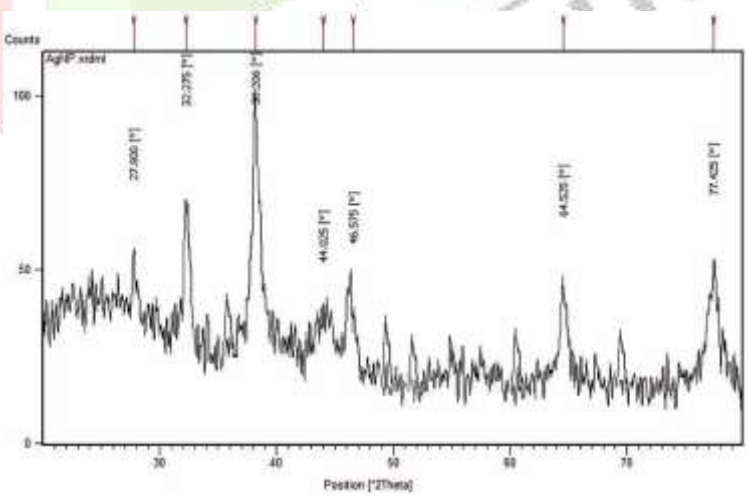

Figure 15XRD pattern of biogenic (*syzygium cumini seed* extract mediated) AgNo3

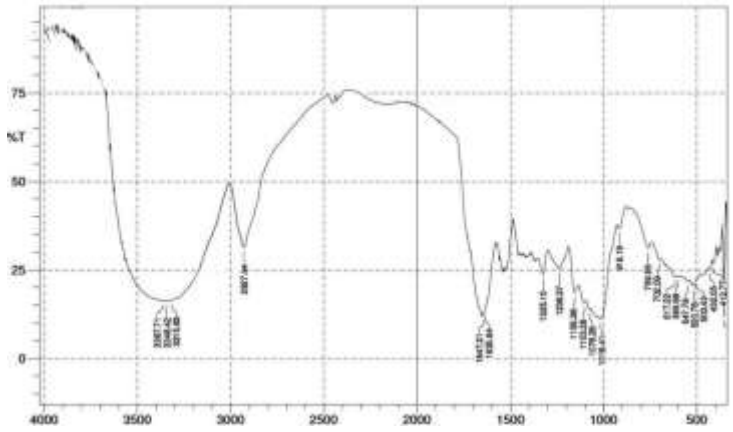

Figure 16 FT-IR spectrum of *syzygium cumini seed AgNo3* extract.

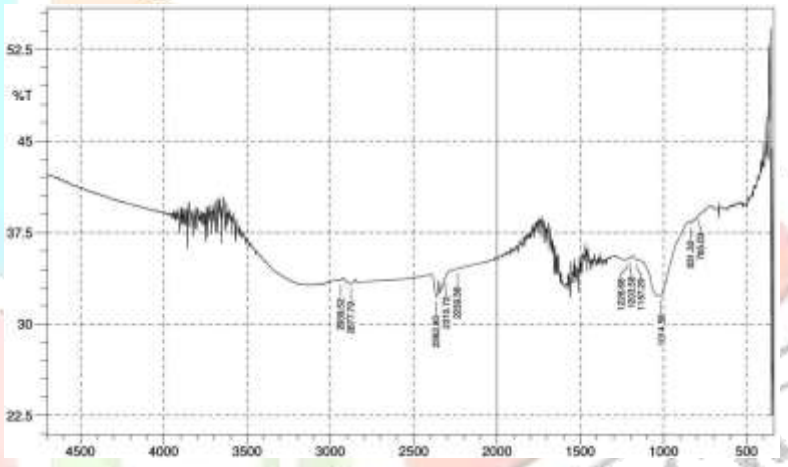

Figure 17 FT-IR spectrum of *syzygium cumini seed* extract mediated biogenic silver nanoparticles.

DISCUSSION

Being a minor Seed, Jamun is having lot of medicinal and pharmaceutical advantages. But it is an unexploited seed. Thus the attempt was made to determine the physicochemical properties of Jamun and explore the nutritive benefits and usefulness of the seed.

Based on this investigation the following conclusions can be drawn on the physical properties of Jamun seed and seed with AgNo3 also about it's at a particular average moisture content of 79.21% (w.b) and 52.24 %(w.b). The frequency distribution curves tends to be a normal distribution. AM and GM are used for determining the volume of the seed as well as the Seed with AgNo3 theoretically. The arithmetic mean diameter (AM) and geometric mean diameter (GM) were 23.9 and 44.8 mm, respectively for the whole seed and 14.6 and 8.7 mm for the seed AgNo3.

CONCLUSION

The present work was designed to investigate the biosorption behavior of Pb and Cd to the blue green alga A. sphaerica. The maximum biosorption capacities were 111.1 mg/g and 121.9 mg/g for Cd(II), Pb(II) and Cr(IV) at optimum operating conditions, respectively. The experimental data revealed that Cd(II), Pb(II) and Cr(IV) biosorption were fitted to both Freundlish and Langmuir isotherms. The mean free energy values calculated from the D–R plot were 11.7 and 14.3 kJ/mol indicating that the biosorption type was chemisorption. The FTIR indicated that the amino, carboxyl, hydroxyl and carbonyl groups on the surface of the biomass are responsible for biosorption of Cd(II), Pb(II) and Cr(IV). Based on these results, SC biomass can be used as an efficient low cost biomass for the removal of heavy metals from wastewater.

REFERENCES

1. Dahiya S., Tripathi R.M., Hegde A.G. Biosorption of heavy metals and radionuclide from aqueous solutions by pre-treated arca shell biomass. J Hazard Mater. 2008;150:376–386. [PubMed]

2. Chen Z., Ma W., Han M. Biosorption of nickel and copper onto treated alga (Undaria pinnatifida): application of isotherm and kinetic models. J Hazard Mater. 2008;155:327–333. [PubMed]

3. Sari A., Tuzen M. Biosorption of Pb(II) and Cd(II) from aqueous solution using green alga (Ulva lactuca) biomass. J Hazard Mater. 2008;152:302–308. [PubMed]

4. Barbier F, Duc G, Petit-Ramel M, Adsorption of lead and cadmium ions from aqueous solution to the montmorillonite: water interface, Colloids Surf., A: Physicochem. Eng. Aspects 2000;166:153–159.

5. Selatnia A., Boukazoula A., Kechid N., Bakhti M.Z., Chergui A., Kerchich Y. Biosorption of lead(II) from aqueous solution by a bacterial dead Streptomyces rimosus biomass. Biochem Eng J. 2004;19:127–135.

6. Hajialigol S., Taher M.A., Malekpour A. A new method for the selective removal of cadmium and zinc ions from aqueous solution by modified clinoptilolite. Adsorp Sci Technol. 2006;24:487–496.

7. Yu Q., Matheickal J.T., Yin P., Kaewsarn P. Heavy metal uptake capacities of common marine macro algal biomass. Water Res. 1999;33:1534–1537.

8. Turker A.R. Separation, preconcentration and speciation of metal ions by solid phase extraction. Sep Purif Rev. 2012;41:169–206.

9. Iyer A., Mody K., Jha B. Biosorption of heavy metals by a marine bacterium. Mar Pollut Bull. 2005;50(3):340–343. [PubMed]

10. Goksungur Y., Uren S., Guvenc U. Biosorption of cadmium and lead ions by ethanol treated waste baker's yeast biomass. Bioresour Technol. 2005;96(1):103–109. [PubMed]

11. Tunali S., Akar T., Ozcan A.S., Kiran I., Ozcan A. Equilibrium and kinetics of biosorption of lead (II) from aqueous solutions by cephalosporium aphidicola. Sep Purif Technol. 2006;47(3):105–112.

12. Anayurt R.A., Sari A., Tuzen M. Equilibrium, thermodynamic and kinetic studies on biosorption of Pb(II) and

Cd(II) from aqueous solution by macrofungus (Lactarius scrobiculatus) biomass. Chem Eng J. 2009;151:255–261. [PubMed]

13. Gupta V.K., Rastogi A. Biosorption of lead(II) from aqueous solutions by non-living algal biomass Oedogonium sp. and Nostoc sp. – a comparative study. Colloids Surf B: Biointerf. 2008;64:170–178. [PubMed]

14. Gupta V.K., Rastogi A. Biosorption of lead from aqueous solutions by green algae Spirogyra species: kinetics and equilibrium studies. J Hazard Mater. 2008;152:407–414. [PubMed]

15. Deng L., Su Y., Su H., Wang X., Zhu X. Biosorption of copper (II) and lead (II) from aqueous solutions by nonliving green algae Cladophora f ascicularis: equilibrium, kinetics and environmental effects. Adsorption. 2006;12:267–277.

16. Gupta V.K., Rastogi A. Biosorption of hexavalent chromium by raw and acid-treated green alga Oedogonium hatei from aqueous solutions. J Hazard Mater. 2009;163:396–402. [PubMed]

17. DÖnmez G., Aksu Z. Removal of chromium (VI) from saline wastewaters by Dunaliella species. Process Biochem. 2002;38:751–762.

18. Chojnacka K., Chojnacki A., Górecka H. Trace element removal by Spirulina sp. from copper smelter and refinery effluents. Hydrometallurgy. 2004;73:147–153.

19. El-Sheekh M.M., El-Shouny W.A., Osman M.E.H., El-Gammal E.W.E. Growth and heavy metals removal efficiency of Nostoc muscorum and Anabaena subcylindrica in sewage and industrial wastewater effluents. Environ Toxicol Pharmacol. 2005;19:357–365. [PubMed]

20. Roy D., Greenlaw P.N., Shane B.S. Adsorption of heavy metals by green algae and ground rice hulls. J Environ Sci Health. 1993;28:37–50.

21. Carmichael WW. Isolation, culture and toxicity testing of toxic fresh water cyanobacteria (blue-green algae). In: Shilo V, editor. Fundamental research in homogeneous catalysis, vol. 3. New York: Gordon& Breach Publ.; 1986. P. 1249.

22. APHA. Standard Methods for the Examination of Water and Wastewater, 21th ed. Washington, DC: American Public Health Association; 2005.

23. Volesky B. Biosorption process simulation tools. Hydrometallurgy. 2003;71:179–190.

24. Murphy V., Hughes H., McLoughlin P. Cu(II) binding by dried biomass of red, green and brown macroalgae. Water Res. 2007;41:731–740. [PubMed]

25. Lodeiro P., Barriada J.L., Herrero R., Sastre de Vicente M.E. The marine macroalga cystoseira baccataas biosorbent for cadmium(II) and lead(II) removal: kinetic and equilibrium studies. Environ Pollut. 2006;142:264–273. [PubMed]

26. Gaur N., Dhankhar R. Removal of Zn+2 ions from aqueous solution using Anabaena variabilis: equilibrium and kinetic studies. Int J Environ Res. 2009;3(4):605–616.

27. King P., Rakesh N., Beenalahri S., Kumar P., Prasad V.S.R.K. Removal of lead from aqueous solution using syzygium cumini L. equilibrium and kinetic studies. J Hazard Mater. 2007;142:340–347. [PubMed]

28. Kaewsarn P. Cadmium biosorption of copper(II) from aqueous solutions bypre-treated biomass of marine

algae Padina sp. Chemosphere. 2002;47:1081–1085. [PubMed]

29. Amini M., Younesi H., Bahramifar N., Lorestani A.A.Z., Ghorbani F., Daneshi A., Sharifzadeh M. Application of response surface methodology for optimization of lead biosorption in an aqueous solution by Aspergillus niger. J Hazard Mater. 2008;154:694–702. [PubMed]

30. Karthikeyan S., Balasubramanian R., Iyer C.S.P. Evaluation of the marine algae Ulvafasciata and Sargassum sp. for the biosorption of Cu(II) from aqueous solutions. Bioresour Technol. 2007;98:452–455. [PubMed]

31. Yin P.H., Yu Q.M., Jin B., Ling Z. Biosorption removal of cadmium from aqueous solution by using pretreated fungal biomass cultured from starch wastewater. Water Res. 1999;33:1960–1963.

32. Su-Hsia L., Ruey-Shin J. Adsorption of phenol and its derivatives from water using synthetic resins and low-cost natural adsorbents: a review. J Environ Manage. 2009;90:1336–1349. [PubMed]

33. Langmuir I. Adsorption of gases on plain surface of glass mica platinum. J Am Chem Soc. 1918;40:1361–1403.

34. Schiewer S, Volesky B. In: Lovely DR, editor. Environmental microbe –metal interactions. Washington, DC: ASM Press; 2000 [chapter 14].

35. Saygideger S., Gulnaz O., Istifli E.S., Yucel N. Adsorption of Cd(II), Cu(II) and Ni(II) ions by Lemna minor L.: effect of physicochemical environment. J Hazard Mater. 2005;126:96–104. [PubMed]

36. El-Shafey E.I. Sorption of Cd(II) and Se(IV) from aqueous solution using modified rice husk. J Hazard Mater. 2007;147:546–555. [PubMed]

37. Tuzen M., Sari A. Biosorption of selenium from aqueous solution by green algae (Cladophora hutchinsiae) biomass: equilibrium, thermodynamic and kinetic studies. Chem Eng J. 2010;158:200–206.

38. Kilislioglu A., Bilgin B. Thermodynamic and kinetic investigations of uranium adsorption on amberlite IR-118H resin. Appl Radiat Isotopes. 2003;50:155–160. [PubMed]

39. Dubinin M.M., Zaverina E.D., Radushkevich L.V. Sorption and structure of active carbons I. Adsorption of organic vapors. Zhurnal Fizicheskoi Khimii. 1947;21:1351–1362.

40. Khan S.A., Rehman U.R., Khan M.A. Adsorption of chromium (III), chromium (VI) and silver (I) on bentonite. Waste Manage. 1995;15:271–282.

41. Smith JM. Chemical engineering kinetics, 3rd ed. New York: McGraw-Hill; 1981. p. 310–22.